Mechanisms and *in vitro* effects of cepharanthine hydrochloride: Classification analysis of the drug-induced differentially-expressed genes of human nasopharyngeal carcinoma cells

GUANJUN LIU[1,3*], DONGMEI WU[1,2*], XINQIANG LIANG[1], HUIFEN YUE[1] and YING CUI[1]

[1]Department of Medical Research, Affiliated Tumor Hospital of Guangxi Medical University, Nanning, Guangxi 530021; Departments of [2]Radiotherapy, and [3]Oncology, Xinxiang Center Hospital, Xinxiang, Henan 453000, P.R. China

Received March 5, 2015; Accepted June 11, 2015

DOI: 10.3892/or.2015.4193

Abstract. Nasopharyngeal carcinoma (NPC) is the most commonly diagnosed head and neck malignancy and is prevalent worldwide. Previous studies have demonstrated the antitumor properties of cepharanthine hydrochloride (CH) in several human cancer cells. However, the action of CH in NPC cells has yet to be determined. In the present study, we investigated the effects of CH in human NPC cell lines including CNE-1 and CNE-2 on cell growth and apoptosis *in vitro*. Using MTT and ATP-tumor chemosensitivity assays it was found that CH inhibited cell viability. Additionally, flow cytometric and analysis electron microscopy revealed the inhibition of cell cycle progression and reduction of apoptosis, respectively, in human NPC cell lines including CNE-1 and CNE-2 *in vitro*. To identify the potential action mechanisms of CH, the cDNA microarray analysis results were confirmed by quantitative PCR analysis using a number of genes, including CDKN1A/P21, NR4A1/TR3 and DAXX. In total, 138 upregulated and 63 downregulated genes in CNE-2 cells were treated with CH. According to their biological function, the genes were classified as: i) cell cycle-related genes; ii) DNA repair-related genes; iii) apoptosis-related genes and iv) nuclear factor-κB (NF-κB) transcription factors signal pathways. The results of the present study showed that CH is a potential therapeutic agent against human NPC, and provide rational explanations and a scientific basis for the study of the development of CH in the treatment of NPC.

Correspondence to: Professor Ying Cui, Department of Medical Research, Affiliated Tumor Hospital of Guangxi Medical University, 71 He Di Road, Nanning, Guangxi 530021, P.R. China
E-mail: ycuigx@139.com

*Contributed equally

Key words: nasopharyngeal carcinoma, cepharanthine hydrochloride, cDNA microarray, cell cycle, DNA repair, apoptosis, nuclear factor-κB signal pathways

Introduction

Nasopharyngeal carcinoma (NPC) is the most common head and neck malignancy with a unique geographical and ethnic distribution, being particularly prevalent in Southern China and Southeast Asia (1). As with most other types of cancers, the prognosis for NPC is strongly associated with the presenting stage (2). Although NPC is extremely radiosensitive (3), metastasis is found in 7% of patients at initial diagnosis and 20% or more develop metastasis following treatment (4). Moreover, the appearance of local or distant relapse determines a less favorable prognosis for these patients (5). Chemotherapy is a crucial treatment for late stage NPC patients; however, the regimen is often not completed due to the severe side effects (6). Chinese traditional medicines have a mild pharmacological action and have been utilized in tumor therapy via naturally occurring drugs (7-10). Cepharanthine hydrochloride (CH) is a biscoclaurine (bisbenzylisoquinoline) amphipathic alkaloid that is isolated from *Stephania cepharantha Hayata* (11). CH has several pharmacological actions, including anti-inflammatory (12), anti-allergic (13) and immunomodulatory activities (14) *in vivo*. In anticancer investigations, CH exhibited multiple pharmacological actions, including potentiating the effects of antitumor agents (15), inducing apoptosis (16,17) and radiation sensitization (18,19), and reversing the multidrug resistance (20-22). However, to the best of our knowlege, no studies have focused on the antitumor effects of CH on NPC.

In the present study, we initially investigated the effects of CH in human NPC cell lines, including CNE-1 and CNE-2, on cell growth and apoptosis *in vitro*, and demonstrated, to the best of our knowledge, for the first time that, CH exerts a potent anti-NPC effect by inhibiting cell growth and inducing apoptosis. To gain a global and deep insight into the molecular mechanisms for the anti-NPC action of CH, we performed cDNA microarray analysis to identify differentially expressed genes in response to CH in CNE-2 cells, which was confirmed by reverse transcriptase-quantitative PCR (RT-qPCR).

Materials and methods

Cell culture and CH treatment. The human CNE-1 and CNE-2 NPC cell lines were grown at 37˚C in 5% CO_2 atmosphere in

Dulbecco's modified Eagle's medium (DMEM) supplemented with 10% fetal bovine serum (both from Gibco, Grand Island, NY, USA), 100 μg/ml penicillin and 100 U/ml streptomycin (Harbin Pharmaceutical Group Co., Ltd., Harbin, China). CH was purchased from the College of Life Science and Technology of Jinan University (Guangzhou, China) and dissolved in a physiologic saline as a stock solution. CNE-1 and CNE-2 cells were treated with various concentrations (5, 10, 20, 40, 60 and 80 mg/l) of CH for the indicated durations (24, 48, 72 and 96 h). Control cells were treated with saline only.

MTT assay. CNE-1 and CNE-2 cells were seeded at a density of $2x10^4$ cells/well in 96-well plates overnight and treated with various concentrations of CH for different periods of time as indicated. Then, 20 μl of 5 mg/ml of 3-(4,5-dimethyl thiazol-2yl)-2,5-diphenyltetrazolium bromide (MTT) (Sigma, St. Louis, MO, USA) was added to each of the culture wells, and the plates were incubated for another 4 h. Following medium removal, 100 μl of DMSO was added to each well and plates were gently agitated for 15 min to dissolve all crystals. Optical absorbance was determined at 490 nm using an ELISA microplate reader (Tecan, Männedorf, Swiss).

ATP-tumor chemosensitivity assay. Cells (100 ml) ($2x10^4$ cells/ml) were seeded in 96-well plates for 24 h at 37˚C with 5% CO_2, and treated with phosphate-buffered saline (PBS) as the control or 50% inhibiting concentration (IC_{50}) of CH (12.5 and 20.0 mg/l for CNE-1 and CNE-2 cells, respectively) for 24-96 h. At the end of the culture period, 50 ml with ATP extraction reagent (DCS Innovative Diagnostik Systeme, Hamburg, Germany) was added to the cells. The 100 μl aliquots of the lysates from each well were transferred into the corresponding wells of the new 96-well plates, and then 20 μl luciferin-luciferase reagent (DCS Innovative Diagnostik Systeme) was added into each well. In addition, we added 120 ml PBS in the blank well as the blank control. The light output corresponding to the level of ATP present was measured in a luminometer (Berthold Technologies, Bad Wildbad, Germany) and the growth inhibition was calculated using the formula: Growth inhibition percentage (%) = $(M_c - M_t)/(M_c - M_b)$ x 100, where M_c, M_t and M_b stand for results of the control, test and blank groups, respectively.

Cell cycle analysis. CNE-1 and CNE-2 cells were treated with saline or the IC_{50} of CH for 48 h, and then collected by centrifugation and rinsed twice with PBS. The cells were fixed in 70% ethanol and centrifuged again. The cells were stained with propidium iodide solution (50 mg/l) containing 1 mg/l of RNase A (both from Sigma) for 30 min at 37˚C. After incubation, the stained cells were rapidly analyzed using a FACScan flow cytometer (BD Biosciences, San Jose, CA, USA).

Electron microscopic analysis of cell apoptosis. Briefly, CNE-1 and CNE-2 cells, which were treated with saline or the IC_{50} of CH for 48 h, were collected and washed twice in 0.1 mol/l phosphate buffer (pH 7.4) by centrifugation. The cell agglomerate of CNE-1 and CNE-2 cells were immersed in 0.1 mol/l phosphate buffer (pH 7.4) with 2.5% glutaraldehyde for 2 h at least, then post-fixed with 1% osmium tetroxide in 0.1 mol/l phosphate buffer (pH 7.0) for 30 min. After dehydration in a graded series of acetonum, the samples were embedded in Epon 812 at room temperature overnight. Ultrathin sections were cut, mounted on copper grids, and stained with uranyl acetate and lead citrate using standard methods. Stained grids were examined and photographed using a transmission electron microscope (TEM) (Hitachi, Toyko, Japan).

cDNA microarray analysis

cDNA microarray construction. The cDNA microarray was manufactured by the Shanghai Biochip Co., Ltd., China. Briefly, the human genes assessed in the present study, contained 16,450 unigenes (including 10-positive control and 6-negative control cDNAs), which were associated with various cell functions and signaling pathways, involving cell cycle, DNA repair, apoptosis, metabolism, cytoskeleton, proinflammatory effect, signaling transduction, and transcription factor.

RNA preparation, reverse transcription, probe construction and hybridization. CNE-2 cells were exposed to saline or IC_{50} CH for 24 h, and total RNA was extracted using a Qiagen RNeasy® kit (Qiagen, Hilden, Germany) according to the manufacturer's instructions. The quality of total RNA was assessed by agarose gel electrophoresis.

During the reaction of cDNA, Cy3/Cy5-dUTP was incorporated into the cDNA of the control and treatment sample, respectively. Briefly, total 10 μl solution including 3 μg random primer and 50 μg of total RNA from untreated and CH-treated cells was added into the PCR tube and degenerated, respectively, at 70˚C for 10 min. Then, 1.0 μl Cy3/Cy5-dUTP (1 mM) (Amersham Biosciences, Piscataway, NJ, USA), 1.0 μl SuperScript II (200 U/ μl) (Invitrogen-Life Technologies, Carlsbad, CA, USA) were added into the tube to construct the reverse transcription reaction system, which was incubated for 2 h at 42˚C, degenerated for 5 min at 70˚C in the dark and terminated by 2 μl NaOH (2.5 M). The probe was purified according to the QIAquick Nucleotide Removal kit (Qiagen), quantified and stored at -20˚C in vacuum.

For hybridization, 30 pmol Cy3/Cy5 labeling probe with a total volume up to 9 μl was added into the tube and degenerated for 3 min at 94˚C. Then, 2 μg human Cot-1 DNA (Invitrogen-Life Technologies) was added into the tube and incubated for 45 min at 70˚C. The previously prepared solution was mixed with 10 μl 4X hybridization solution and 20 μl methylamine to a final volume of 40 μl. Hybridization was titrated in microarray and carried out at 42˚C for 16-18 h in the dark and moist box. Following completion of hybridization, the microarray was washed with 1X SSC/0.2% SDS wash buffer for 10 min at 55˚C, 0.1X SSC/0.2% SDS wash buffer for 10 min at 55˚C twice, 0.1X SSC wash buffer for 5 min twice and ddH_2O for 2 min at room temperature, and was dried by centrifugation at 1,500 rpm for 5 h.

Microarray data analysis. Microarray images from two-color fluorescent hybridization were scanned with an Agilent scanner (Agilent Technologies, Inc., Santa Clara, CA, USA). The scanning results were analyzed using ImaGene software (BioDiscovery, Hawthorne, CA, USA), and normalized using GeneSpring software; Silicon Genetics, Redwood City, CA, USA). Fluorescent images were gridded to locate the spot

Table I. The primer sequences of each checked gene and its PCR production length.

Gene name	Primer sequence	Length (bp)
GAPDH	F: TGACTTCAACAGCGACACCCA R: CACCCTGTTGCTGTAGCCAAA	121 (954-1,074)
CDKN1A	F: CAGCGACCTTCCTCATCCA R: GACTCCTTGTTCCGCTGCTAA	71 (1,697-1,767)
NR4A1	F: CTCATATGCCACCCCATGTG R: TGGAGTCATTCTGCAGCTCAA	159 (2,207-2,165)
DAXX	F: AAGAGCCCCATGTCCTCACTAC R: CTCCCCTGAAGATCTGCTGATC	81 (1,595-1,675)

F, forward; R, reverse.

corresponding to each gene. Raw gene expression data were generated for each gene. The fold-change of each probe was calculated from the two dye-swap arrays, and the probes with ≥2-fold change in one assay and ≤0.5-fold in its dye-swap were considered to have a statistically significant change in gene expression.

Clustering analysis was carried out to classify the differentially expressed genes based on the similarity of the functions using GeneSpring software. The order can be observed according to the functions of differentially expressed genes.

RT-qPCR. The same batches of total RNA from untreated and CH-treated CNE-2 cells for cDNA microarray were utilized for the synthesis of first-strand cDNA. The specific primer sequences and the expected amplicon size for GAPDH, CDKN1A, NR4A1 and DAXX are shown in Table I. RT-qPCR was performed using a SYBR-Green reaction mixture in the ABI 7300 detection system (Applied Biosystems, Foster City, CA, USA). The amplification program used was: one cycle at 50˚C for 2 min and 95˚C for 10 min; followed by 40 cycles at 95˚C for 15 sec and 60˚C for 1 min. The gene expression data were normalized to the endogenous control GAPDH. The relative gene expression levels were measured according to the formula $2^{-\Delta\Delta Ct}$. The samples were run in triplicate and repeated twice.

Statistics analysis. SPSS software version 18.0 (SPSS, Inc., Chicago, IL, USA) was used for all statistical analyses by means of t-test, factor analysis and one-factor analysis of variance. The data in the tables and figures were publicized in the form of mean or mean ± standard deviation (SD). $P<0.05$ was considered to indicate a statistically significant result.

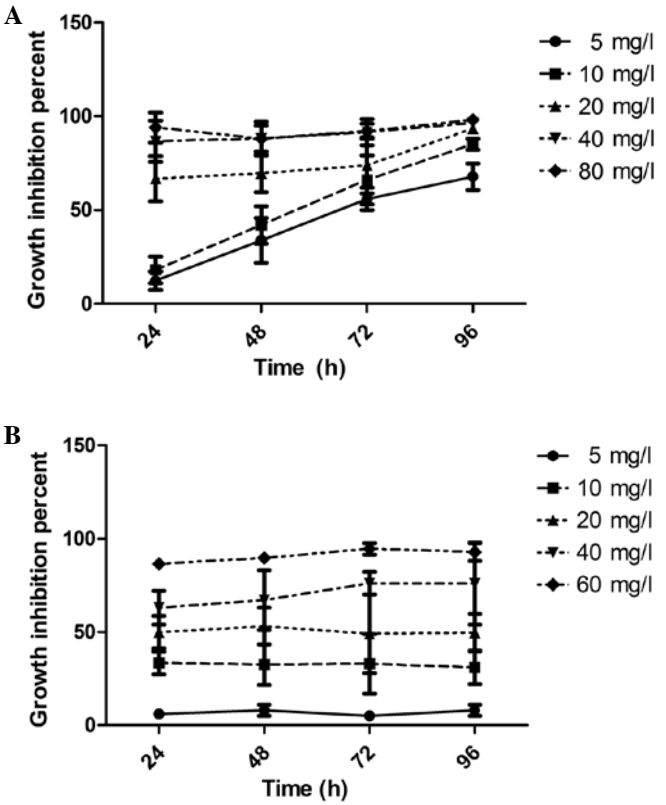

Figure 1. (A) The curve of the inhibition of CNE-1 treated with different concentrations of CH over four days. (B) The curve of the inhibition of CNE-2 treated with different concentrations of CH over four days. CH, cepharanthine hydrochloride.

Results

Effects of CH on cell growth. After CNE-1 and CNE-2 cells were exposed to CH at various concentrations ranging from 5.0 to 80 mg/l for 24-96 h, cell viability was determined using the MTT assay. We observed that CNE-1 cells treated with CH presented a dose- and time-dependent decrease in cell viability when compared with the untreated cells (Fig. 1A). CNE-2 cells exhibited a dose- but not time-dependent effect in response to CH ranging from 5.0 to 60.0 mg/l (Fig. 1B). The median IC_{50} values of CH for CNE-1 and CNE-2 cells calculated after 48 h treatment were 12.5 and 20.0 μg/ml, respectively. To confirm the cytotoxic effect of CH, we performed an ATP-tumor chemosensitivity assay to determine the inhibition ratio (IR) of CNE-1 and CNE-2 cells in response to IC_{50} of CH for 24-96 h. The data (Table II) were in accordance with the MTT results. These results indicated that CH effectively inhibited CNE-1 and CNE-2 cell growth.

Effects of CH on cell cycle progression. To determine whether CH impaired the cell cycle of CNE-1 and CNE-2 cells, flow

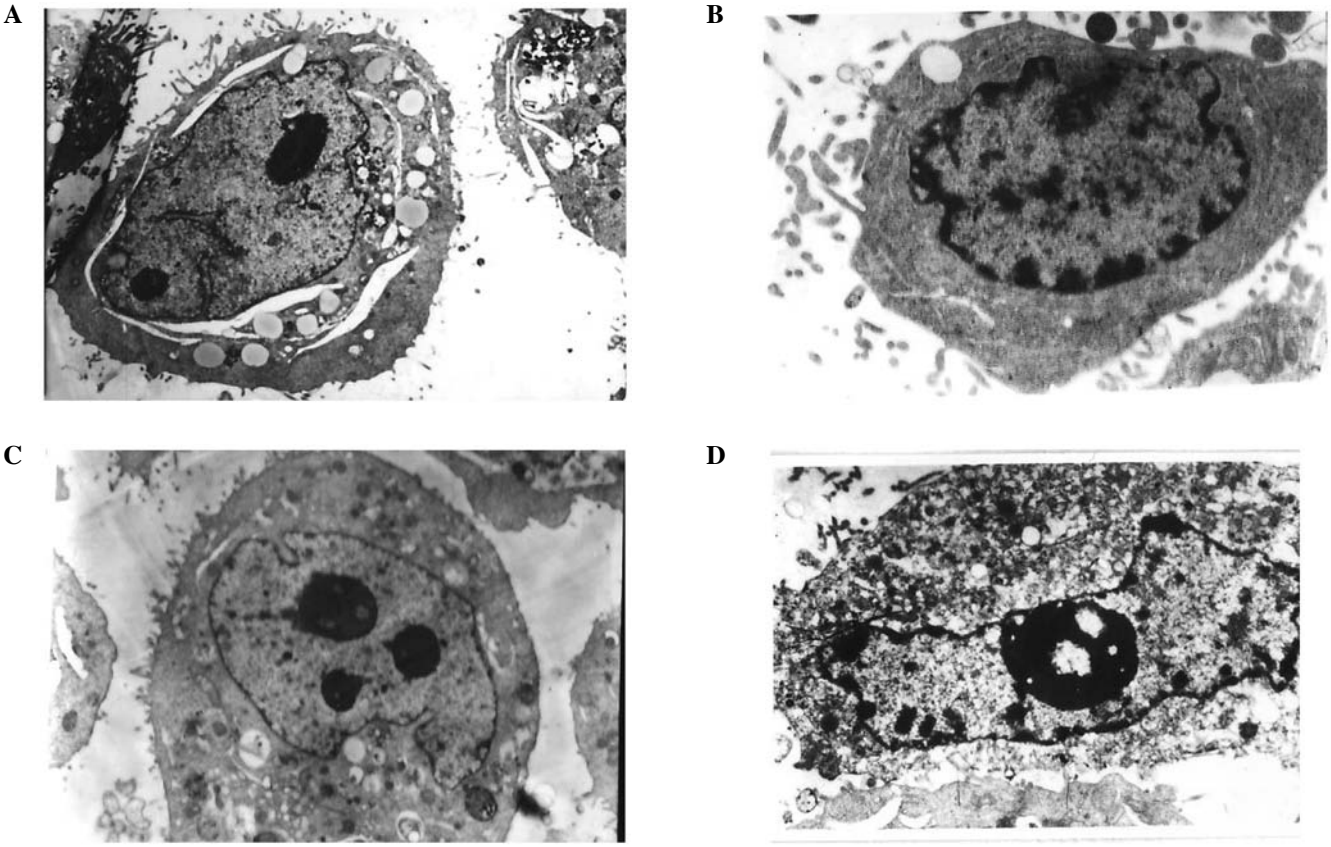

Figure 2. TEM micrographs of CNE-1 and CNE-2 cells treated (A and C) without and with (B and D) IC_{50} CH value for two days. (A and C) Untreated CNE-1 (magnification, x5,000) and CNE-2 cells (magnification, x5,000), showing typical ultrastructure characterized by a well-preserved plasma membrane. Abundant microvilli are visible on the surface, and the nucleus became larger and contained a nucleolus and euchromatin. (B) Early stage of apoptosis CNE-1 (magnification, x5,000). Most organelles in the cytoplasm lost some of their individual characteristics, few microvilli are visible on the cell surface, and the main ultra-microstructural changes are chromatin aggregation are visible on the periphery of the nucleus. (D) Apoptotic characteristics of CNE-2 (magnification, x5,000). Few microvilli are visible on the cell surface, with more extensive nuclear chromatin condensation, fragmentation of nuclei and formation of apoptotic bodies being observed. TEM, transmission electron microscope; CH, cepharanthine hydrochiorid.

Table II. The inhibition ratio (IR) of CNE-1 and CNE-2 cells in response to IC_{50} of CH.

Cells	24 h IR (%)	48 h IR (%)	72 h IR (%)	96 h IR (%)
CNE-1	27.7±5.2	50.1±9.5	64.9±4.3	73.7±3.0
CNE-2	44.5±4.6	50.9±2.9	55.0±4.8	54.4±11.4

CH, cepharanthine hydrochloride; IR, inhibition ratio.

cytometry was employed to examine the distribution of the cell cycle. As shown in Table III, 48 h after treatment with IC_{50} of CH apparently retarded CNE-1 and CNE-2 cells to enter the S phase. This result clearly suggested that the growth inhibitory effect of CH in CNE-1 and CNE-2 cells resulted from cell cycle arrest in the G_1 phase.

Effects of CH on cell apoptosis. TEM, which is one of the best methods to observe cell morphology including cytoplasm, organelle and nuclei, was used to confirm apoptosis of CNE-1 and CNE-2 cells treated with PBS or with IC_{50} of CH for 48 h. As shown in Fig. 2A and C, there were no typical morphological changes indicative of apoptosis in the controls of CNE-1 and CNE-2 cells. By contrast, when CNE-1 and CNE-2 cells were exposed to IC_{50} of CH for 48 h, typical apoptotic morphological changes were observed (Fig. 2B and D).

cDNA microarray profile of CNE-2 cells in response to CH. To gain a global understanding of the pharmacological mechanism of CH in NPC cells, the cDNA microarray technique was used to establish the gene expression profiles of CNE-2 cells untreated or treated with CH. Signals were invisible in the blank spots, while the housekeeping gene density was similar, indicating that the results were credible. Preliminary results showed that the expression levels of 499 genes were significantly altered by CH in CNE-2 cells (Fig. 3). After rejecting some complicated data, we found that there were 144 upregulated and 63 downregulated genes in the CH-treated CNE-2 cells. According to their attributes and functions in the biological processes, these differentially expressed genes may be classified as: i) cell cycle-related, ii) DNA repair-related, iii) apoptosis-related genes, and iv) nuclear factor-κB (NF-κB) transcription factors signal pathways. The segmental different genes associated with growth inhibition are shown in Table IV.

RT-qPCR analysis of several differentially expressed genes. To verify the data gained from cDNA microarray, three interesting genes, i.e., CDKN1A (NM_000389), NR4A1 (NM_002135)

Table III. The cell cycle influence of IC_{50} CH on CNE-1 and CNE-2 cells.

Groups	Cell cycle			Proliferation index (%)
	G_0/G_1 (%)	S (%)	G_2/M (%)	
Control group of CNE-1	42.0±12.7	46.0±10.1	12.0±2.6	58.00
Experimental group of CNE-1	70.9±10.7[a]	22.9±7.9[a]	6.1±2.1[a]	29.03
Control group of CNE-2	40.3±6.7	45.7±3.8	13.9±3.0	59.66
Experimental group of CNE-2	74.4±5.7[a]	18.2±6.2[a]	7.3±2.2[a]	25.53

[a]P<0.05 vs. the corresponding control group. CH, cepharanthine hydrochloride.

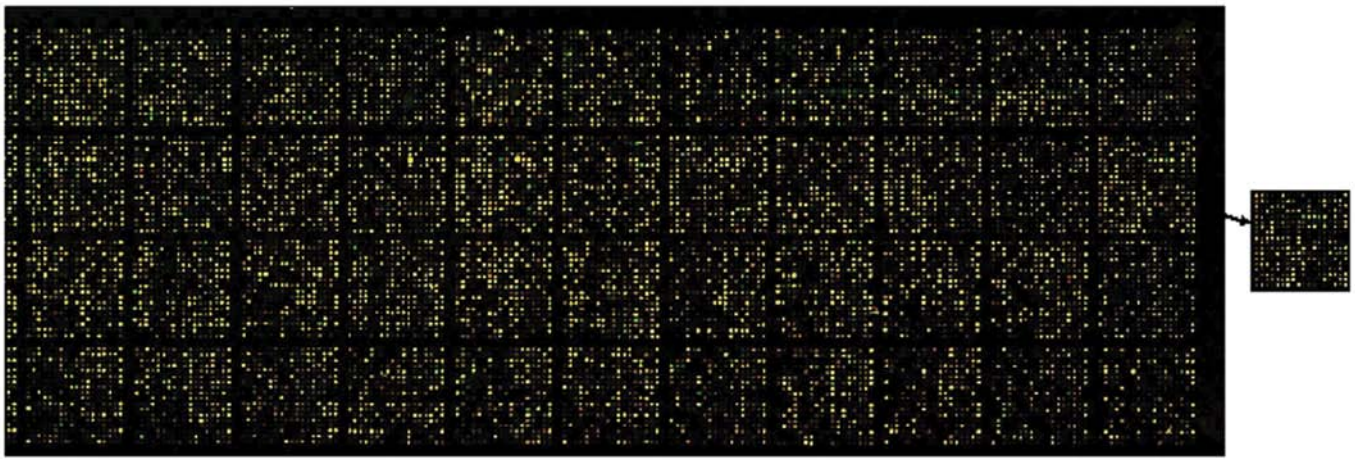

Figure 3. Overlay of Cy3/Cy5 double-marked fluorescence. Green and red points are down- and upregulated genes, respectively.

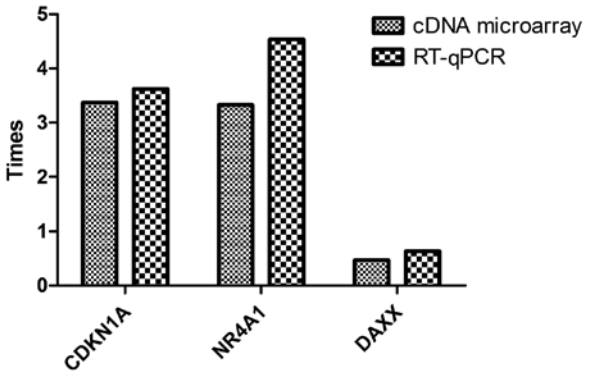

Figure 4. The comparison of CDKN1, NR4A1, DAXX between cDNA microarray and RT-qPCR.

and DAXX (NM_001350) (function and mapping information are presented in Table V), were selected for RT-qPCR analysis. As shown in Table VI and Fig. 4, although some variability on the individual gene expression changes existed, a consistent differential expression trend was evident in the results from cDNA microarray and those from RT-qPCR.

Discussion

Nasopharyngeal carcinoma (NPC) is the most common head and neck malignancy within southern China and southeast Asia. Chemotherapy is crucial for late stage NPC patients. Nevertheless, treatment is often not completed due to the serious side effects caused (6). Chinese traditional medicines, which possess an anticancer function have been utilized in tumor therapy via naturally occurring drugs. Cepharanthine hydrochloride (CH), which is known as a membrane-interacting agent that has membrane-stabilizing activity, is a biscoclaurine alkaloid extracted from the roots of *Stephania cepharantha Hayata* and possesses plenty pharmacological activities (12-14). Evidence suggests that CH potentiates the activity of certain anticancer agents (15-17) and restores the effect of anticancer drugs in multidrug/radioresistant cancer cells (18-22). In the present study, we investigated whether CH affected CNE-1 and CNE-2 cell growth. The results show that there was a dose- and time-dependent decrease on the CNE-1 cell treated with CH, whereas only dose-dependent relationships were identified with CNE-2. At the same time, we assessed the effects of CH on the growth of CNE-1 and CNE-2 cells by means of an ATP-tumor chemosensitivity assay, the results of which were consistent with those of the MTT assay. Carcinomas are known to undergo an uncoordinated proliferation. Thus, we carried out cell cycle analysis and cell apoptosis detection. The results show that CH retarded the cell cycle and promoted the apoptosis of CNE-1 and CNE-2 cells. Tumor proliferation is associated with numerous growth regulatory genes in a multistep process of carcinogenesis and neoplasm progression. Gene expression is able to characterize the

adaptation of cells to changes in an external environment and is also a sensitive indicator of toxicant exposure. To examine the intimate pharmacological molecular mechanism of the anti-NPC of CH, using cDNA microarray we identified that CH functions by cell cycle-related genes such as CDKN1A, ID1, CCNF, UNG2 and CBX7; DNA repaired-related genes such as XRCC1, RAD51L3 and NCOA6; and apoptosis-related genes such as NR4A1, DAXX, GADD45α, TNFRSF10b and DFFB. The results of RT-qPCR are consistent with the results of the cDNA microarray in the expression of differential genes (including CDKN1A, NR4A1 and DAXX) and show that the results of cDNA microarray are credible.

Cell cycle association genes. The cell division cycle is an important factor regulating cancer growth. In normal cells, the division cycle has been divided into G_1, S, G_2 and the M phases. Cells that do not divide are deemed to be in the G_0 phase. When cells receive external stimulation to initiate division, they changed from the quiescent state into the cell division. A basic strategy when evaluating anticancer drugs is to arrest the cell cycle. In the present study, we found that CH of the 48 h IC_{50} arrested the CNE-1 and CNE-2 cells from entering S phase and interfering with the proliferation of CNE-1 and CNE-2 cells when compared to the untreated cells. The cell cycle control system includes the cyclin-dependent kinases (CDKs), cyclins and cycle-dependent kinases inhibitors (CDKIs). The interactions of CDKs and cyclins can induce cell division; however, CDKIs inhibit the cell cycles. As shown in Table IV, we found upregulation of the proliferation stimulator (for example CDKN1A and CDKN2B) and downregulation of the proliferation inhibitor (for example ID1, CCNF, UNG2 and CBX7) in our investigation plays a direct role in CNE-1 cell proliferation following CH treatment.

p21, which is known as a cyclin-dependent kinase inhibitor 1 or CDK-interacting protein 1, is a protein that is encoded by the *CDKN1A* gene located on chromosome 6 (6p21.2) in humans. The p21 protein binds to and inhibits the activity of cyclin-CDK2 or -CDK4 complexes, and thus functions as a regulator of cell cycle progression at G_1 phase (22,23). The expression of this gene is closely controlled by the tumor suppressor protein p53, through which this protein mediates the p53-dependent cell cycle G_1 phase arrest in response to a variety of stress stimuli (22,23). In our experiment, we identified the overexpression of p21 by cDNA microarray in NPC cells treated with CH. Thus, p21 inhibits the proliferation of NPC cells treated with CH.

ID1 gene is a type of downregulation of the proliferation inhibitor that was found by cDNA microarray. The ID1 gene encodes a type of positive regulator, a helix-loop-helix (HLH) protein that forms heterodimers with members of the basic HLH family of transcription factors and inhibits the DNA binding and transcriptional activation ability of basic HLH proteins with which it interacts. Evidence has shown that ID1 is able to promote cell proliferation and cell cycle progression through the inactivation of tumor suppressor pathways (24). In addition, the overexpression of ID1 suppresses the expression of p21 by means of the bond with its promoter-E box (25). The downregulation of ID1 is able to block the proliferation of NPC cells treated with CH. The mechanisms of p21 under the control of ID1 and E box may play a vital role in the arrest of NPC cells treated with CH.

Table IV. The segmental genes associated with growth inhibition in different genes.

Classification	Gene bank	Gene	Ratio
Cell cycle association genes	BC014469	CDKN2B	2.071
	NM_000389	CDKN1A	3.374
	NM_000576	IL1B	4.933
	NM_000600	IL6	8.1
	NM_002199	IRF2	3.611
	NM_003244	TGIF	2.19
	NM_004235	KLF4	2.659
	NM_006568	CGRRF1	2.162
	X54489	CXCLL	26.42
	NM_002615	SERPINF1	0.443
	NM_021147	UNG2	0.452
	NM_001761	CCNF	0.391
	NM_002467	MYC	2.15
	NM_006190	ORC2L	3.187
	NM_003842	TNFRSF10B	2.064
	L24498	GADD45A	12.36
DNA repair association genes	NM_006297	XRCC1	0.476
	NM_021147	UNG2	0.452
	NM_014071	NCOA6	0.416
	NM_002878	RAD51L3	0.471
	NM_002135	NR4A1	3.238
	NM_001350	DAXX	0.467
	L24498	GADD45A	12.36
	NM_015675	GADD45B	4.892
Cell apoptosis association genes	BC014469	CDKN2B	2.071
	NM_000389	CDKN1A	3.374
	NM_003842	TNFRSF10B	2.064
	NM_004760	STK17A	2.702
	NM_004341	CAD	2.994
	NM_001964	EGR1	2.012
IκB/NF-κB signaling pathway	NM_006290	TNFAIP3	2.991
	NM_006622	PLK2	4.665
	NM_018290	NALP12	3.87
	NM_004760	STK17A	2.702
	NM_003244	TGIF	2.19
	AL133012	CHUK	2.097
	NM_024039	MIS12	2.064
	Z57391	HIP14L	2.051

DNA repair association genes. In the process of cell division, the human stable genome guarantees smooth cell proliferation. On the other hand, unstable genome is characteristic of cancer cells and accelerates broken and deformed chromosomes in the process of cancer cell division. If genetic abnormalities cannot be repaired, cell cycle restraint or apoptosis is triggered in the process of cancer cell division. DNA repair-related genes are employed to correct such drawbacks. In the present study, we found CH induces the downregulation of DNA repair genes

Table V. Function and mapping information of the three genes selected for validation.

Gene name	Gene bank	Chromosome	Function
CDKN1A	NM_000389	6p21.2	A potent cyclin-dependent kinase inhibitor
NR4A1/TR3	NM_002135	12q13	A member of the steroid/thyroid/retinoid nuclear receptor superfamily and regulation of growth and apoptosis
DAXX	NM_001350	6p21.3	Linking the death receptor to the c-Jun amino-terminal kinase pathway

Table VI. Ct and ratio of each checked gene.

	Control group			Test group			
Genes	Ct	ΔCt	$2^{-\Delta Ct}$	Ct	ΔCt	$2^{-\Delta Ct}$	Times ($2^{-\Delta\Delta Ct}$)
GAPDH	11.9584			11.9574			
CDKN1A	18.4303	6.4719	0.01126585	20.2867	8.3293	0.003109073	3.623540452
NR4A1	18.8283	6.8699	0.008549762	21.0091	9.0517	0.001884373	4.537192908
DAXX	19.9025	7.9441	0.004060576	19.2424	7.285	0.006412044	0.63327323

such as XRCC1, RAD51L3 and NCOA6. The XRCC1 gene encoded a protein that is involved in the efficient repair of DNA single-strand breaks formed by exposure to ionizing radiation and alkylating agents. This protein interacts with DNA ligase III, polymerase β and poly(ADP-ribose) polymerase to participate in the DNA repair pathway (26). The RAD51L3 gene is another downregulated gene derived from DNA repair genes. It encodes a member protein of the RAD51 protein family that is known to be involved in the homologous recombination and repair of DNA. This protein forms a complex with several other members of the RAD51 family, including RAD51L1, RAD51L2 and XRCC2. The protein complex formed with this protein has been shown to catalyze homologous pairing between single- and double-stranded DNA, and is thought to play a role in the early stage of recombinational repair of DNA (27). We consider that downregulation of the DNA repair genes such as XRCC1, RAD51L3 and NCOA6, is associated with the functions of CH in NPC cells. Following treatment of NPC cells with CH, upregulation of the proliferation stimulator (for example CDKN1A and CDKN2B) and downregulation of the proliferation inhibitor (for example ID1, CCNF, UNG2 and CBX7) may play a direct role in the inhibition of NPC cell proliferation and block NPC cell cycles by their signal pathway. In the process of cell cycle arrest, the damaged DNA of NPC cells induced by CH need to be repaired and escape the checkpoint of cell cycles. However, the downregulation DNA repair association genes inhibits DNA repair and proliferation, and cell apoptosis association genes via CH induce NPC cell apoptosis.

Cell apoptosis association genes. The word 'apoptosis' comes form the Greek word meaning 'falling leaves' and was first used to describe a new form of cell death distinct from necrosis. Apoptosis is the morphologic appearance of programmed cell death which is an important mechanism in embryonic development, neurodegenerative diseases and homeostasis (28). However, the dysregulated apoptosis is a crucial step in tumorigenesis (28). Concerning cancer therapy, the ultimate purpose of cytotoxic therapies is to induce apoptosis or death of tumor cells. In the present study, typical apoptotic morphological changes were observed in these cells when the cells were exposed to IC_{50} CH for 48 h. This showed the ability of CH to induce apoptosis. The process of apoptosis involves numerous genes. We found CH induces the expression of apoptotic genes (for example NR4A1, DAXX, GADD45α and TNFRSF10b).

NR4A1 is a member of the steroid/thyroid/retinoid nuclear receptor superfamily. During apoptosis, NR4A1 expression is rapidly induced and plays roles in regulating growth and apoptosis in cancer cells. NR4A1 binding to the Bcl-2 N-terminal loop region and resulting in a conformational change in Bcl-2 can convert Bcl-2 from a protector to a killer protein (29). In the present study, we found that the expression of NR4A1 in NPC cells treated with CH was 3.238- and 4.537-folds, respectively, compared with the control group in the cDNA microarray test and RT-qPCR. The overexpression of NR4A1 plays an important role in the apoptosis of NPC cells treated with CH.

DAXX, which links the death receptor to the c-Jun amino-terminal kinase pathway, is another protein associated with apoptosis. DAXX negatively regulates apoptosis at the early embryonic stages (30) and cancer cells (31) via the p53 pathway. The downregulation of DAXX induced by CH may be one of the pathways leading to apoptosis in NPC cells.

GADD45, which responds to environmental stresses and the anticancer activity of chemotherapeutic agents, is an apoptosis-related gene mediated by p53 and the p53 homologues in our study. After DNA is damaged, the GADD45 protein family members are induced rapidly, participate actively in DNA repair mechanisms, and result in cell cycle arrest and/or apoptosis (32). Evidence has also been provided that drug therapies act to directly or indirectly upregulate GADD45α

and GADD45β and promote cancer cell apoptosis. In the present study, we found that CH induces the upregulation of GADD45α and GADD45β in NCP cells. As GADD45α and GADD45β are essential components of numerous metabolic pathways that control proliferation and induce cancer cell apoptosis, they may be regarded as emerging drug targets in NPC cells treated with CH.

Nuclear factor-κB transcription factor signaling pathways. Nuclear factor-κB (NF-κB) transcription factor signaling pathways are central components of immune responses and inflammatory. Evidence suggests that NF-κB signaling pathways that are involved in its activation are also important for tumor development. NF-κB is a negative regulator of cell proliferation (33) and a positive activator of anti-apoptotic genes (34). TNFAIP3 is a key negative regulator of the NF-κB signal, through a wide variety of cell surface receptors and viral proteins. Previous findings have shown that TNFAIP3 reduces cell proliferation (35) and induces the apoptosis of cancer treated with chemotherapeutics (36-38). In the present study, similar results were obtained whereby TNFAIP3 was upregulated by CH, reduced proliferation and induced NPC cell apoptosis.

In conclusion, to the best of our knowledge, we report for the first time that CH inhibited cell proliferation and induced apoptosis in NPC cells. The cDNA microarray analysis revealed that the anti-NPC action of CH may be mediated by regulating the expression levels of a variety of genes involved in cell cycle regulation, DNA repair, cell apoptosis and the NF-κB signaling pathway. Our findings provide a rational and scientific basis for the further study and development of CH as a potentially useful agent for NPC therapy, although more in-depth investigations are required.

Acknowledgements

This study was supported by the National Natural Science Foundation of China (grant no. 30660203), the Applied Basic Special Research Program of Science and Technology Department of Guangxi Zhuang Autonomous Region (grant no. 0731062), and Innovation Program of Guangxi Graduate Education.

References

1. Jemal A, Bray F, Center MM, Ferlay J, Ward E and Forman D: Global cancer statistics. CA Cancer J Clin 61: 69-90, 2011.
2. Wang J, Huang Y, Guan Z, Zhang JL, Su HK, Zhang W, Yue CF, Yan M, Guan S and Liu QQ: E3-ligase Skp2 predicts poor prognosis and maintains cancer stem cell pool in nasopharyngeal carcinoma. Oncotarget 5: 5591-5601, 2014.
3. Lin JC, Jan JS, Hsu CY, Liang WM, Jiang RS and Wang WY: Phase III study of concurrent chemoradiotherapy versus radiotherapy alone for advanced nasopharyngeal carcinoma: Positive effect on overall and progression-free survival. J Clin Oncol 21: 631-637, 2003.
4. Chang YH, Wu CC, Chang KP, Yu JS, Chang YC and Liao PC: Cell secretome analysis using hollow fiber culture system leads to the discovery of CLIC1 protein as a novel plasma marker for nasopharyngeal carcinoma. J Proteome Res 8: 5465-5474, 2009.
5. Lee AW, Poon YF, Foo W, Law SC, Cheung FK, Chan DK, Tung SY, Thaw M and Ho JH: Retrospective analysis of 5037 patients with nasopharyngeal carcinoma treated during 1976-1985: Overall survival and patterns of failure. Int J Radiat Oncol Biol Phys 23: 261-270, 1992.
6. Lin HX, Hua YJ, Chen QY, Luo DH, Sun R, Qiu F, Mo HY, Mai HQ, Guo X, Xian LJ, *et al*: Randomized study of sinusoidal chronomodulated versus flat intermittent induction chemotherapy with cisplatin and 5-fluorouracil followed by traditional radiotherapy for locoregionally advanced nasopharyngeal carcinoma. Chin J Cancer 32: 502-511, 2013.
7. Lo LC, Chen CY, Chen ST, Chen HC, Lee TC and Chang CS: Therapeutic efficacy of traditional Chinese medicine, Shen-Mai San, in cancer patients undergoing chemotherapy or radiotherapy: Study protocol for a randomized, double-blind, placebo-controlled trial. Trials 13: 232, 2012.
8. Li X, Chen T, Lin S, Zhao J, Chen P, Ba Q, Guo H, Liu Y, Li J, Chu R, *et al*: Valeriana jatamansi constituent IVHD-valtrate as a novel therapeutic agent to human ovarian cancer: In vitro and in vivo activities and mechanisms. Curr Cancer Drug Targets 13: 472-483, 2013.
9. Hou X, Yuan X, Zhang B, Wang S and Chen Q: Screening active anti-breast cancer compounds from Cortex *Magnolia officinalis* by 2D LC-MS. J Sep Sci 36: 706-712, 2013.
10. Su CC: Tanshinone IIA potentiates the efficacy of 5-FU in Colo205 colon cancer cells in vivo through downregulation of P-gp and LC3-II. Exp Ther Med 3: 555-559, 2012.
11. Lv JJ, Xu M, Wang D, Zhu HT, Yang CR, Wang YF, Li Y and Zhang YJ: Cytotoxic bisbenzylisoquinoline alkaloids from *Stephania epigaea*. J Nat Prod 76: 926-932, 2013.
12. Kudo K, Hagiwara S, Hasegawa A, Kusaka J, Koga H and Noguchi T: Cepharanthine exerts anti-inflammatory effects via NF-κB inhibition in a LPS-induced rat model of systemic inflammation. J Surg Res 171: 199-204, 2011.
13. Goto M, Zeller WP and Hurley RM: Cepharanthine (biscoclaurine alkaloid) treatment in endotoxic shock of suckling rats. J Pharm Pharmacol 43: 589-591, 1991.
14. Furusawa S and Wu J: The effects of biscoclaurine alkaloid cepharanthine on mammalian cells: Implications for cancer, shock, and inflammatory diseases. Life Sci 80: 1073-1079, 2007.
15. Kono K, Takahashi JA, Ueba T, Mori H, Hashimoto N and Fukumoto M: Effects of combination chemotherapy with biscoclaurine-derived alkaloid (Cepharanthine) and nimustine hydrochloride on malignant glioma cell lines. J Neurooncol 56: 101-108, 2002.
16. Takahashi-Makise N, Suzu S, Hiyoshi M, Ohsugi T, Katano H, Umezawa K and Okada S: Biscoclaurine alkaloid cepharanthine inhibits the growth of primary effusion lymphoma in vitro and in vivo and induces apoptosis via suppression of the NF-kappaB pathway. Int J Cancer 125: 1464-1472, 2009.
17. Harada T, Harada K and Ueyama Y: The enhancement of tumor radioresponse by combined treatment with cepharanthine is accompanied by the inhibition of DNA damage repair and the induction of apoptosis in oral squamous cell carcinoma. Int J Oncol 41: 565-572, 2012.
18. Tamatani T, Azuma M, Motegi K, Takamaru N, Kawashima Y and Bando T: Cepharanthin-enhanced radiosensitivity through the inhibition of radiation-induced nuclear factor-κB activity in human oral squamous cell carcinoma cells. Int J Oncol 31: 761-768, 2007.
19. Zahedi P, De Souza R, Huynh L, Piquette-Miller M and Allen C: Combination drug delivery strategy for the treatment of multidrug resistant ovarian cancer. Mol Pharm 8: 260-269, 2011.
20. Li H, Yan Z, Ning W, Xiao-Juan G, Cai-Hong Z, Jin-Hua J, Fang M and Qing-Duan W: Using Rhodamine 123 accumulation in $CD8^+$ cells as a surrogate indicator to study the P-glycoprotein modulating effect of cepharanthine hydrochloride in vivo. J Biomed Biotechnol 2011: 281651, 2011.
21. Peng YM, Wang N, Wang YF, Han L, Zhang Y, Jiang JH, Zhou YB and Wang QD: Correlation between reversing effect of cepharanthine hydrochloride on multidrug resistance and P-glycoprotein expression and function of K562/ADR cells. Yao Xue Xue Bao 47: 594-599, 2012 (In Chinese).
22. Abbas T and Dutta A: p21 in cancer: Intricate networks and multiple activities. Nat Rev Cancer 9: 400-414, 2009.
23. Liu G and Lozano G: p21 stability: Linking chaperones to a cell cycle checkpoint. Cancer Cell 7: 113-114, 2005.
24. Geng H, Rademacher BL, Pittsenbarger J, Huang CY, Harvey CT, Lafortune MC, Myrthue A, Garzotto M, Nelson PS, Beer TM, *et al*: ID1 enhances docetaxel cytotoxicity in prostate cancer cells through inhibition of p21. Cancer Res 70: 3239-3248, 2010.
25. Prabhu S, Ignatova A, Park ST and Sun XH: Regulation of the expression of cyclin-dependent kinase inhibitor p21 by E2A and Id proteins. Mol Cell Biol 17: 5888-5896, 1997.

26. Okano S, Lan L, Tomkinson AE and Yasui A: Translocation of XRCC1 and DNA ligase IIIalpha from centrosomes to chromosomes in response to DNA damage in mitotic human cells. Nucleic Acids Res 33: 422-429, 2005.
27. Suwaki N, Klare K and Tarsounas M: RAD51 paralogs: Roles in DNA damage signalling, recombinational repair and tumorigenesis. Semin Cell Dev Biol 22: 898-905, 2011.
28. Fuchs Y and Steller H: Programmed cell death in animal development and disease. Cell 147: 742-758, 2011.
29. Lin B, Kolluri SK, Lin F, Liu W, Han YH, Cao X, Dawson MI, Reed JC and Zhang XK: Conversion of Bcl-2 from protector to killer by interaction with nuclear orphan receptor Nur77/TR3. Cell 116: 527-540, 2004.
30. Michaelson JS, Bader D, Kuo F, Kozak C and Leder P: Loss of Daxx, a promiscuously interacting protein, results in extensive apoptosis in early mouse development. Genes Dev 13: 1918-1923, 1999.
31. Tang J, Qu LK, Zhang J, Wang W, Michaelson JS, Degenhardt YY, El-Deiry WS and Yang X: Critical role for Daxx in regulating Mdm2. Nat Cell Biol 8: 855-862, 2006.
32. Tamura RE, de Vasconcellos JF, Sarkar D, Libermann TA, Fisher PB and Zerbini LF: GADD45 proteins: Central players in tumorigenesis. Curr Mol Med 12: 634-651, 2012.
33. Dajee M, Lazarov M, Zhang JY, Cai T, Green CL, Russell AJ, Marinkovich MP, Tao S, Lin Q, Kubo Y, *et al*: NF-kappaB blockade and oncogenic Ras trigger invasive human epidermal neoplasia. Nature 421: 639-643, 2003.
34. Karin M and Lin A: NF-kappaB at the crossroads of life and death. Nat Immunol 3: 221-227, 2002.
35. Sakakibara S, Espigol-Frigole G, Gasperini P, Uldrick TS, Yarchoan R and Tosato G: A20/TNFAIP3 inhibits NF-κB activation induced by the Kaposi's sarcoma-associated herpesvirus vFLIP oncoprotein. Oncogene 32: 1223-1232, 2013.
36. Al-Romaih K, Somers GR, Bayani J, Hughes S, Prasad M, Cutz JC, Xue H, Zielenska M, Wang Y and Squire JA: Modulation by decitabine of gene expression and growth of osteosarcoma U2OS cells in vitro and in xenografts: Identification of apoptotic genes as targets for demethylation. Cancer Cell Int 7: 14, 2007.
37. Daigeler A, Chromik AM, Geisler A, Bulut D, Hilgert C, Krieg A, Klein-Hitpass L, Lehnhardt M, Uhl W and Mittelkötter U: Synergistic apoptotic effects of taurolidine and TRAIL on squamous carcinoma cells of the esophagus. Int J Oncol 32: 1205-1220, 2008.
38. Daigeler A, Klein-Hitpass L, Chromik MA, Müller O, Hauser J, Homann HH, Steinau HU and Lehnhardt M: Heterogeneous in vitro effects of doxorubicin on gene expression in primary human liposarcoma cultures. BMC Cancer 8: 313, 2008.